EFFECTS OF DIFFERENTIAL AXIAL SHORTENING ON OUTRIGGER SYSTEMS IN HIGH RISE BUILDINGS WITH CONCRETE FILLED STEEL TUBE COLUMNS

Dilrukshie I. Samarakkody[1]*, David P Thambiratnam[1]
Tommy H.T. Chan[1] and Praveen H.N. Moragaspitiya
[1]School of Civil Engineering and Built Environment,
Queensland University of Technology, 2-George Street, Brisbane, Australia.
*Email: d.samarakkodyarachchilage@hdr.qut.edu.au

ABSTRACT

Concrete Filled Steel Tube (CFST) columns are popular in high rise buildings due to their superior strength, seismic and fire resistance capacities and construction simplicity. Structural framing systems in high rise buildings are commonly coupled with reinforced concrete outrigger and belt systems to facilitate lateral load resistance. When axial shortenings of vertical elements occur due to time dependent phenomena of creep, shrinkage and elastic deformations, the horizontal stiff elements balance the shortening differentials in the vertical elements and cause load redistributing among them dynamically. This can result in high transfer stresses induced in the stiff outrigger and belt systems which need to be considered in design or mitigated during construction. To plan mitigation strategies such as the time to connect the shear core to the structural frame to effectively reduce time dependent transfer stresses, it is necessary to quantify current and future differential axial shortenings. This paper first quantifies the differential axial shortening (DAS) between the shear core and columns, considering effects of construction sequence, time dependent material properties and reinforcement and then quantifies the transfer stresses built up in outrigger and belt systems in CFST high rise buildings. This information will be useful in mitigating the adverse effects of these high transfer stresses.

KEYWORDS

Concrete Filled Tubes, Creep, Elastic deformation, Time Dependent structural performance.

INTRODUCTION

Concrete Filled Steel Tube (CFST) columns have been successfully used in many high rise buildings such as the Taipei 101 tower in Taipei, the Two Union Square in Seattle USA, Shimizu Super High Rise Building in Tokyo, Guangzhou New TV Tower, China and 111 Eagle street, Australia. Axial shortenings of these structural components occur due to time dependent phenomena of basic creep, shrinkage and elastic deformation. Due to different gravity loads supported by these load bearing components they undergo differential settlements.

The structural systems in high rise buildings, with either reinforced concrete or CFST columns are commonly coupled with reinforced concrete outrigger and belt systems for lateral load resistance due to the unique combination of architectural flexibility and structural efficiency they offer compared to tubular systems. The outrigger and belt systems that link the core system to the column are therefore displaced by differential movements which can result in high transfer stresses in the lateral resistance system. In some cases these transfer forces are believed to amount up to the forces generated by the applied design lateral loads (Choi *et al*. 2012).

Although outrigger systems have been extensively used, one area that needs further investigation is the effects of differential shortening on these systems and the accurate prediction of these effects (Choi *et al*. 2012). Research will enhance the understanding in this area and will provide engineers some guidance on the following: (i) feasibility of changing and delaying the entire construction cycle times, (ii) using delayed connection of outrigger belt systems and planning connection times considering the risk of adverse lateral loading events that could occur during construction and (iii) determining the need for or effectiveness of detailed control measures such as sliding friction joints at the intersection of the walls as used in the Water Front Place Brisbane, Australia or damped outriggers developed by ARUP (Choi *et al*. 2012) or design the outrigger and belt systems to the combined effects of lateral loads and differential axial shortening while designing the structural frame system for possible load redistributions.

The accuracy of the predictions of the outrigger transfer stresses and construction planning inevitably depends on the accuracy of the differential axial shortening predictions. Therefore it is important to conduct the axial shortening analysis with adequate detail. The factors that need to be considered are accurate inclusion of the time dependent properties of creep and shrinkage and corresponding loading conditions, global structural effects caused by specific members such as outriggers, raking columns and transfers, effect of construction sequence on the deflection and importantly concrete levelling during construction (Moragaspitiya *et al*. 2010). In addition, previous research on reinforced concrete structural components confirmed that load migration occurs between concrete and steel due to the creep and shrinkage and this has significant effects on the axial shortening of these components (Wang *et al*. 2008) in which the effects of reinforcement need to be considered. This study incorporates all these in the numerical procedure that was developed and applied to quantify axial shortening of CFST columns and shear core walls. This comprehensive procedure can hence be used to accurately predict the stresses developed in the outrigger system due the interactive differential shortenings and control in the high rise structure caused by these horizontal rigid structural components.

METHODOLOGY

A comprehensive and rigorous methodology has been developed in this research incorporating all the time dependent phenomena occurring in the real-life situations. The methodology is based on material models presented in Euro code2 (EC2) which are well established among the practicing engineers and the finite element technique (FET). The creep calculation included in the methodology is based on the Age Adjusted Effective Modulus method (AAEM) developed by Trost and Bazant (Bazant and Baweja 2000) which includes the aging of concrete and can be applied to analyse high rise building accurately with limited computational demand. This combination was selected based on the outcomes of the previous research by Geng et al (Geng *et al*. 2012) who compared several creep material models, except that in AS3600, with results of 81 experimental tests on creep and shrinkage behaviour of CFST for a range of normal and high strength concretes. They used the largest test data on CFSTs and recommended the use of EC2 for the axial shortening predictions and the use of AAEM with coefficients suggested by Bazant and Baweja (Bazant and Baweja 2000).

Creep and Shrinkage Model of Concrete

Creep and shrinkage material models presented in EC2 have been incorporated into the methodology developed and presented in this paper through MPCHG command in the ANSYS finite element code. This command changes the material number attributes of the elements to include the relevant age adjusted elastic modulus value at the considered time step as the material elastic modulus for both column and shear wall elements. In the creep calculation, time-dependent concrete behaviour is modelled by the age adjusted effective modulus method developed by Trost and Bazant (Bazant and Baweja 2000). The age adjusted effective modulus; $\overline{E_c}(t,t_0)$ at any time t for first loading at t_0, is expressed by Equation (1). The aging coefficient; $\chi(t,t_0)$ as defined by Trost and Bazant is in Equation (2) and relaxation function $R(t,t_0)$ in Equations (3) and (3.1).

$$\overline{E_c}(t,t_0)=\frac{E_c(t_0)}{1+\chi(t,t_0)\ \phi(t,t_0)} \tag{1}$$

$$\chi(t,t_0)=\frac{E(t_0)}{E(t_0)-R(t,t_0)}-\frac{1}{\phi(t,t_0)} \tag{2}$$

$$R(t,t_0)=\frac{0.992}{J(t,t_0)}-\frac{0.115}{J_0}\left[\frac{J(t_0+\zeta,t_0)}{J(t,t-\zeta)}-1\right] \tag{3}$$

$$J(t,t_0)=\frac{1}{E_c(t_0)}+\frac{\phi(t,t_0)}{1.05\times E_{ci}} \tag{3.1}$$

Where; t_0 is the time of first loading, $E_c(t_0)$ is the Young's modulus of elasticity at the time of first loading, $\phi(t,t_0)$ is the creep coefficient from EC2 as presented below in Equation (4), $E_{ci}=E_{c0}[f_{cm28}/f_{cm0}]^{0.3}$, $E_{c0}=2.2\times10^4$, $f_{cm0}=10$, $\xi=(t-t_0)/2$ and $J_0=J(\xi+t_0,\xi+t_0-1)$

The creep coefficient; $\phi(t,t_0)$ as obtained from EC2 recommendation gives (BSI, Eurocode2 2004):

$$\phi(t,t_0)=\phi_{RH}\cdot\beta(f_{cm28})\cdot\beta(t_0)\cdot\beta(t-t_0) \tag{4}$$

where ϕ_{RH} , $\beta(f_{cm28})$ and $\beta(t_0)$ are factors to allow for the effects of relative humidity, concrete strength and concrete age at loading on the notional creep coefficient,

$\beta(t-t_0)=\left[\frac{(t-t_0)}{(\beta_H+t-t_0)}\right]^{0.3}$ is the time function of creep development that depends on relative humidity and notional member size $h_0=\frac{2A_c}{u}$ (A_c-concrete cross-sectional area, u is exposed perimeter).

Concrete shrinkage comprises of two components: drying $\varepsilon_{cd}(t)$and autogenous $\varepsilon_{ca}(t)$. The drying shrinkage depends on the notional size, environmental conditions such as relative humidity and temperature, strength of concrete and type of cement used while the autogenous shrinkage depends only on the strength of concrete.

The drying shrinkage component can be represented by Equation (5) below, while the autogenous shrinkage component is as given in Equation (6) below.

$$\varepsilon_{cd}(t)=\beta_{ds}(t,t_s)\cdot k_h\cdot\varepsilon_{cd,0} \tag{5}$$

$$\varepsilon_{ca}(t)=\beta_{as}(t)\cdot\varepsilon_{ca}(\infty) \tag{6}$$

In drying shrinkage, the basic shrinkage strain $\varepsilon_{cd,0}$ is modified with k_h, a coefficient depending on the notional size h_0 and the time function for drying shrinkage $\beta_{ds}(t,t_s)$. Whereas in autogenous shrinkage $\varepsilon_{ca}(\infty)$ *and* $\beta_{as}(t)$ are the basic autogenous shrinkage strain and the time function for shrinkage development respectively.

The procedure developed and presented in this paper uses an infinite value for the hypothetical thickness or notional size of the CFST components in order to eliminate drying components in both shrinkage and creep, which do not influence the axial shortening of CFST. Also, the relative humidity has been considered as 100% to account for the non-exposure of the concrete to the outer environment due to the presence of the steel tube.

The computational technique including the material modal presented above has been validated using experimental data published on Kwon et al (Kwon *et al*. 2005) which presents outcomes of the axial shortening behaviour of CFST columns. Details on the validation are reported elsewhere (Samarakkody *et al*. 2014).

FEM of the High Rise Building

The 60 storey CFST building in this study comprises of a reinforced concrete core shear wall system and belt and outrigger systems which are commonly used in high rise buildings. The building lay out is shown in Figure 2. 80MPa concrete (mean compressive strength at 28 days based on cylinder strength) has been used for outrigger and belt systems, 65MPa concrete has been used for the walls and 40 MPa concrete has been used for the floor plates (thickness -200mm). The reinforcement content of the walls is 3% of the cross sectional area. Sizes of the structural components are presented in Tables 1 and 2. "D" and "t" in Table 1 are the external diameter and the steel tube thickness of CFST columns respectively.

Table 1 Sizes of columns and thicknesses of core shear walls

Floor number	CFST column sizes D x t (mm)	Shear Wall thickness (m)
1-21	1150 x 16	1.2
22-41	900 x 12	1.0
42-60	800 x 8	0.75

Table 2 Size of walls of outrigger and belt systems

Floor number	Outrigger wall size (m)
20-21	0.8
40-41	0.6

The analyses have been conducted incorporating the influences of the self-weight, superimposed dead load (1.8 kPa) and live load (2.5 kPa) and environmental conditions such as 50% humidity (for RC components) and 30^{0}C temperature. A finite element model has been developed for the structural framing system shown in Figure 1. In this model, the columns and beams have been modelled using BEAM188 elements while the shear core walls, slabs and the outrigger- belt system have been modelled using SHELL181 elements.

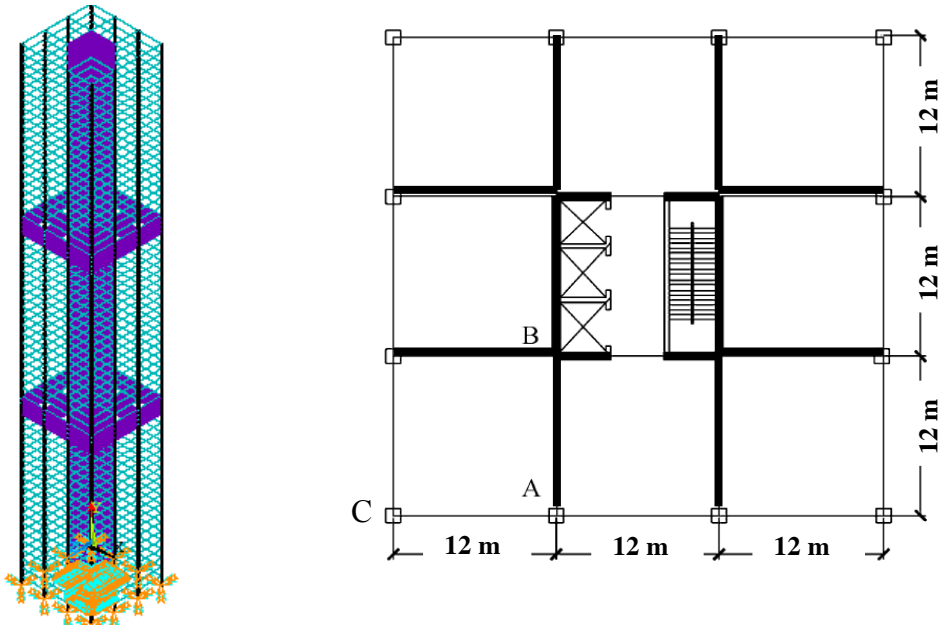

Figure 1 High rise building Isometric View (left) Plan View (right)

Simulation of Construction Sequence

During construction stage of building, structural components are incorporated into the whole structural system following the construction schedule and hence the stiffness and the self-weight for the system vary during construction. “Birth and Death of elements” option with geometric nonlinearity available in ANSYS is utilised to simulate these construction stages accurately. At the beginning of the analysis, all components of the system are killed (or deactivated) and all degrees of freedom (DOF) of these floating elements are fixed. The structural components are then gradually added (activated) according to the construction sequence while releasing the relevant DOF.

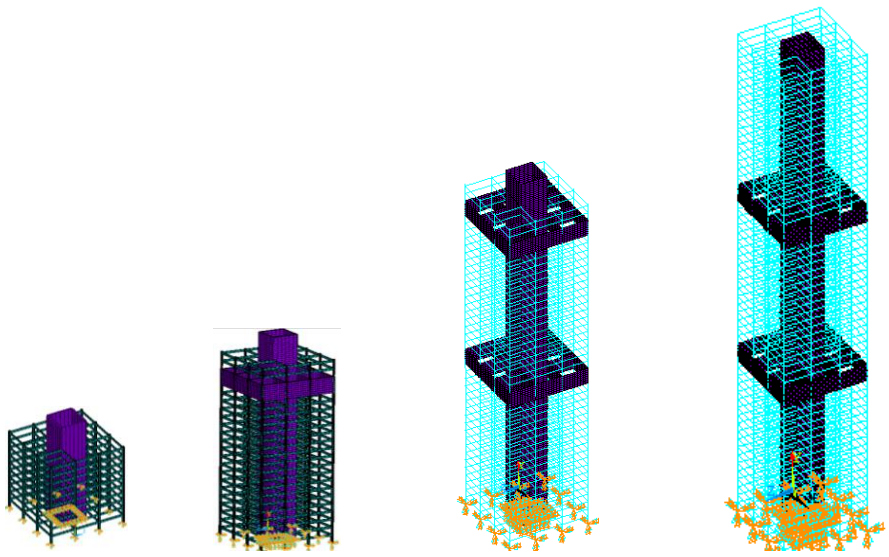

Figure 2 Modelling construction sequence

To achieve the "element death" effect in the ANSYS program, the stiffness of the structural components is multiplied by a very high reduction factor. Element loads associated with deactivated elements are zeroed (removed) out of the load vector. An element's strain is also set to zero when the element is killed. Similarly when an element is reactivated, all these return to their full original values. In addition, elements are reactivated with no record of strain history (ANSYS 2010). Figure 2 above shows the activated elements in a few representative construction steps such as after the construction of (a) 10th story, (b) 23rd story, (c) 43rd story and (d) 60th story.

RESULTS AND DISCUSSIONS

Time dependent behaviour of structural components during and after the construction has been studied. The variation of elastic, creep and shrinkage strains in the CFST column C (Figure 1) at levels 10, 30 and 50 are shown in Figure 3. The EC2 concrete creep modal for these columns predicted a maximum creep coefficient of 0.76, as opposed to the creep coefficient range of 2.0 to 3.0 for normal strength concrete. The present value seems to be close to that observed in the experiments of Uy (Uy 2001) who obtained an average creep coefficient value of 1.0, while testing 6 HSCFT column specimens with concrete having a 28 days compressive strength of 52 MPa. Further, Yisuo Ma (Ma and Wang 2012) observed maximum final creep coefficients of 0.75 and 0.57 at the age of 126 days for specimens with compressive strengths of 75.5 MPa and 85.5 MPa respectively which is closer to the concrete grade of 80 used for the columns in the structural system analysed and presented in this paper. Moreover, the maximum shrinkage strain obtained by EC2 for the CFST columns was 150 micro strains which is comparable with the tests of Uy et al (Uy 2001). After 140 days, they observed a total shrinkage strain of 160 micro strains, for the composite column as opposed to that of 600 micro strains of concrete cylinders which then approached a plateau after 140 days of results. The information above highlights the accuracy of the material models and computational technique used in the analysis.

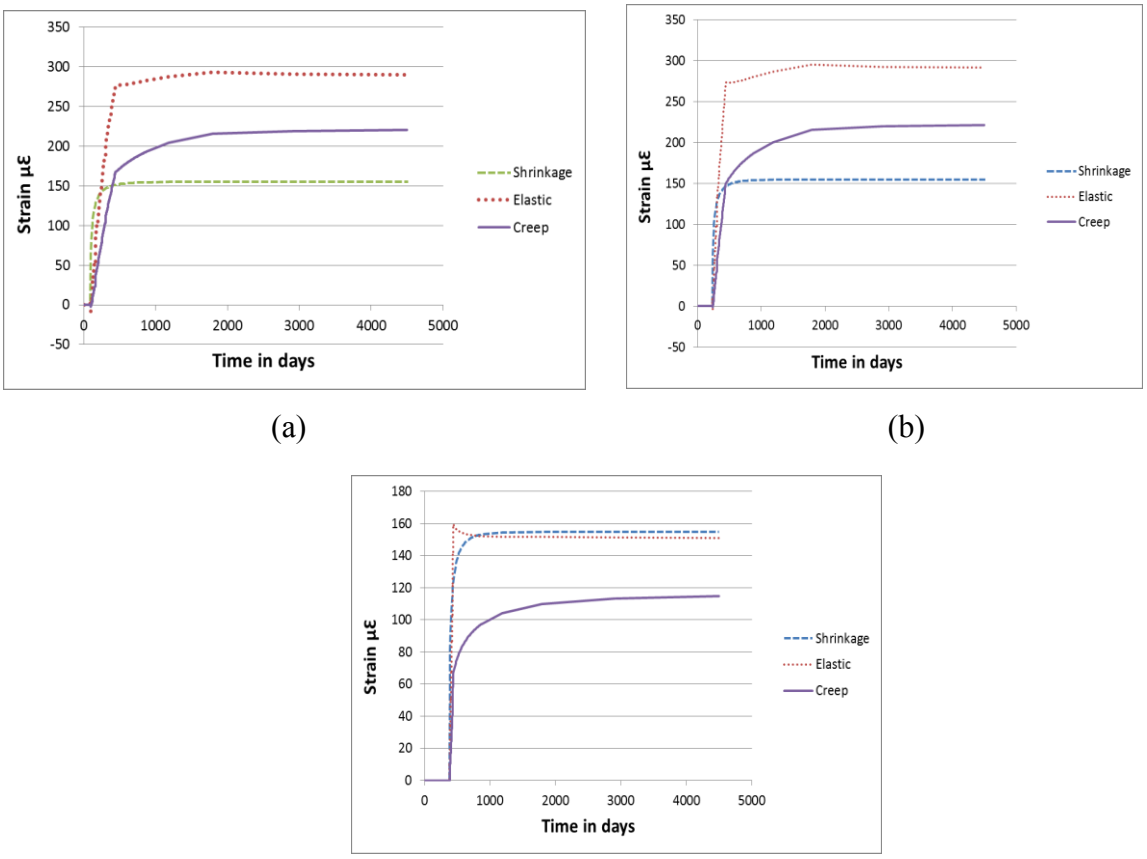

Figure 3 Variation of elastic, creep and shrinkage strains in column C for level (a) 10, (b) 30 and (c) 50

The axial shortening due to time dependent elastic, creep and shrinkage strains of CFST columns and the reinforced concrete shear core walls along the building height are presented in Figure 4. Figure 4(a) and 4(b) show the axial shortening of the CFST column on grids A and C together with the Shear walls at point B (see Figure 1) at each storey level of the building at 483 days (end of construction) and after 4500 days from start of construction respectively. As shown in these Figures, the axial shortening of the column at storey 32 (with a maximum of 51.48 mm) is higher than that of the walls with a maximum value of 44mm at storey 45 due to the fact that the gravity load tributary area of the column is higher compared to that of the walls. However, axial shortening of the top most three storeys of shear wall surpasses that of columns due to higher shrinkage and creep of the reinforced concrete shear wall resulting from drying and the columns being lightly loaded than at the lower levels. The axial shortening of the vertical load bearing structural components are equal at the outrigger floor levels of 19-21 and 39-41 as indicated in Figure 4 confirming that the load migration between the structural components at these locations occurs due to the outrigger systems.

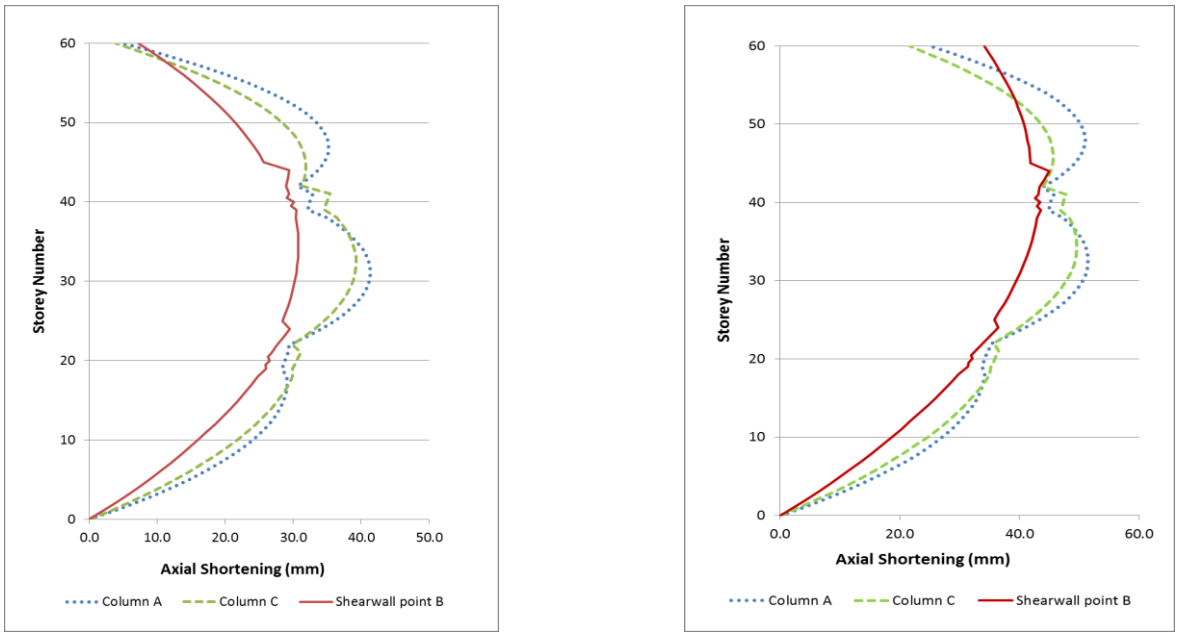

Figure 4 Axial shortening of vertical load bearing elements (a) at the end of construction, (b) at 4500 days from start of construction

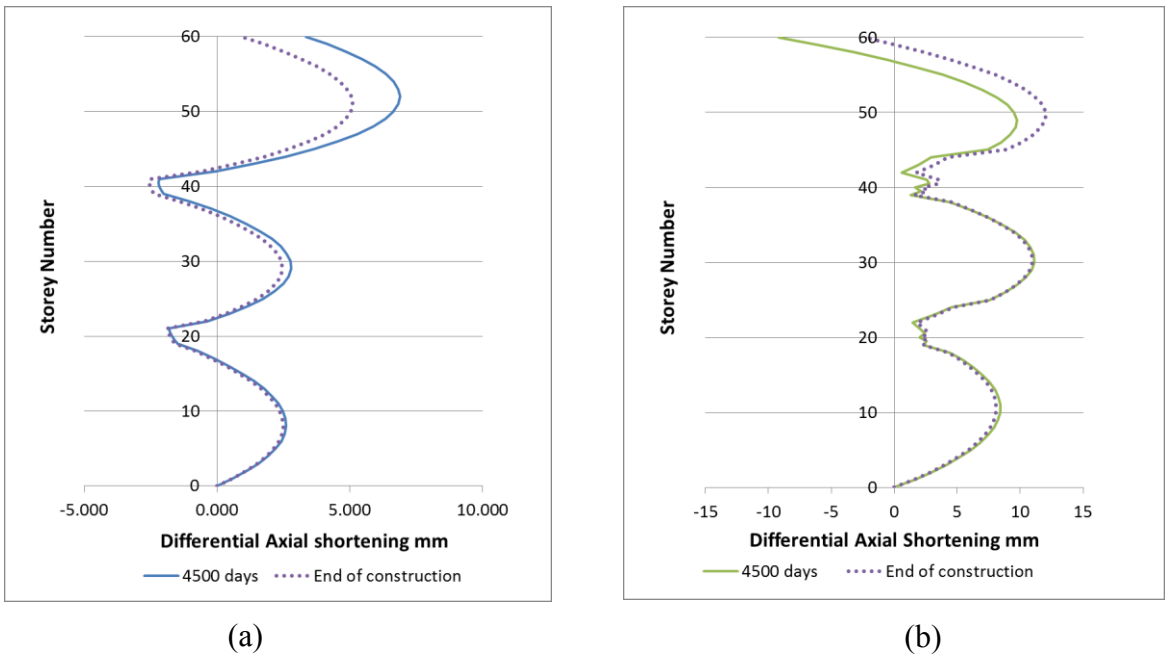

Figure 5 Differential Axial shortening (a) between column A and C, (b) between column A and shear wall at B

Differential Axial shortening between the CFST columns A and B is presented in Figure 5(a) and that between the shear core and the columns linked to it by outrigger is given in Figure 5(b). The maximum differential shortening is about 12mm which is at level 50 of the building and is between the shear core walls and the column connected to it. As evident from the above Figures, differential shortening between the two columns increases with time while that between the perimeter column and shear wall connected with outriggers decreases with the time and reverse in direction due to the load migration occurring through the outrigger and the higher creep and shrinkage occurring in shear walls due to drying.

The above mentioned linkage between columns and shear walls through the outrigger which leads to partial gravity load transfer from columns to shear walls, results in controlling the differential shortening between the structural components. As a result, the outrigger and belt systems are subjected to high gravity transfer stresses. The stress increment due to the load migration, impacts significantly on the performance of the lateral load resisting system of the whole building. This increment is evident in the stress plots in Figure 6 and 7 shown below. Figure 6 (a) and (c) illustrate the horizontal membrane stresses and (b) and (d), the transverse shear stresses of the bottom outrigger located between floor levels 19-21. The first on each set shows the stresses at the end of outrigger construction and the next shows the stresses at the end of 4500 days from the start of construction. Similarly Figure 7 (a), (b), (c) and (d) illustrate these stress distributions for the top outrigger located between floor levels 39-41.

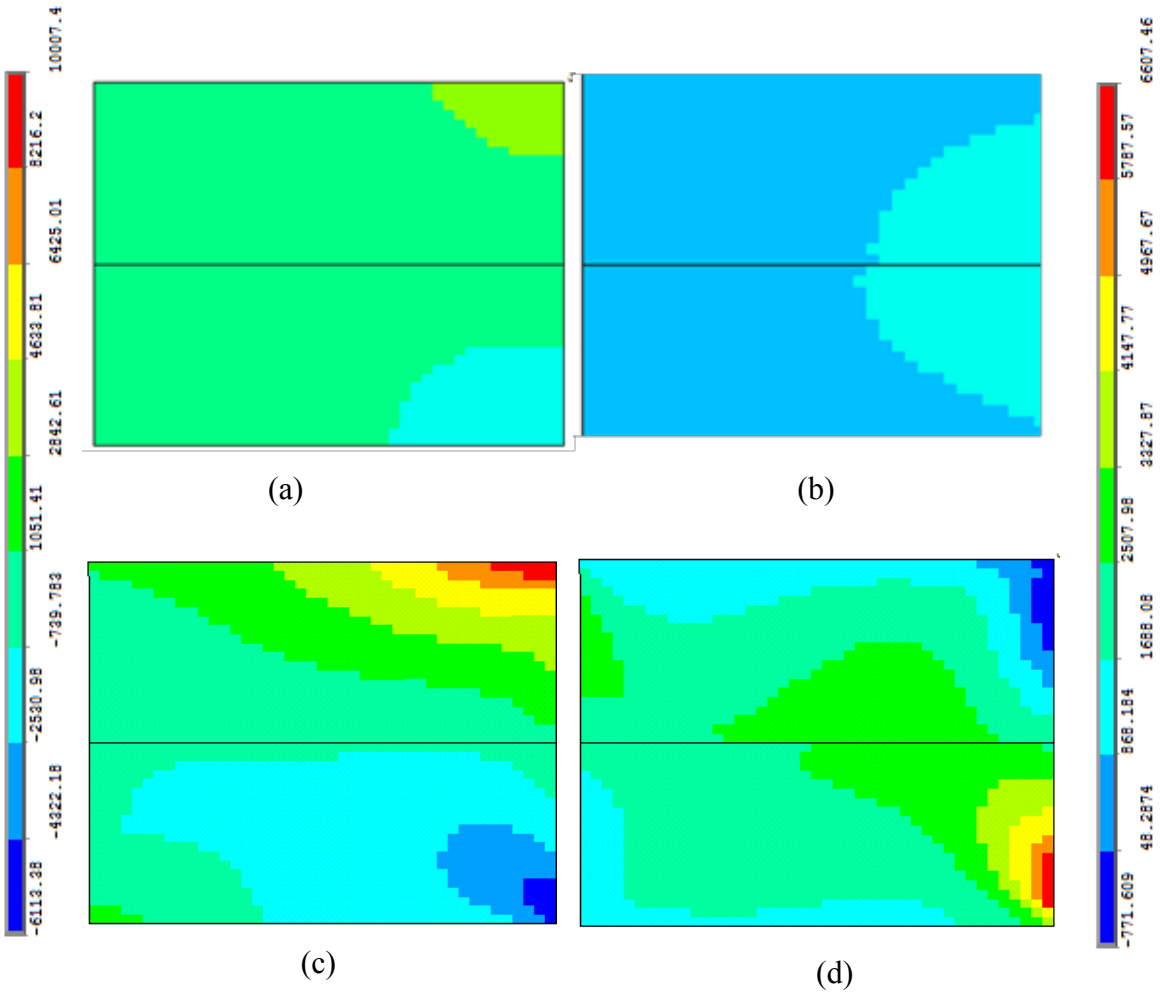

Figure 6 (a) Horizontal membrane stresses, (b) transverse shear stresses at the end of construction of outrigger and (c) horizontal membrane stresses, (d) transverse shear stresses at 4500 days of the bottom outrigger in kN/m^2

Figure 6 illustrates that the maximum horizontal membrane stress of the bottom of the outrigger increases from 2.3MPa (at end of construction) to 10 MPa (after 4500 days) which is an increase of 335%. The transverse shear stresses also increases from 1.3 MPa to 6.6 MPa during the time from removal of formwork of outrigger till end

of 4500 days. Correspondingly the top outrigger horizontal membrane stresses and transverse shear stresses increased by 381% and 340% respectively each rising from 2.451 MPa to 11.8 MPa and 1.57 MPa to 6.9 MPa. Therefore for the specific building considered, there is a 3-4 times increment in outrigger stresses from construction till end of 4500 days due to differential axial shortening of vertical load bearing elements. However, considering the outrigger concrete strength which is 80MPa, the final stresses due to gravity loading and the differential axial shortening are about 14% of the concrete strength therefore doesn't exceed the safety limits.

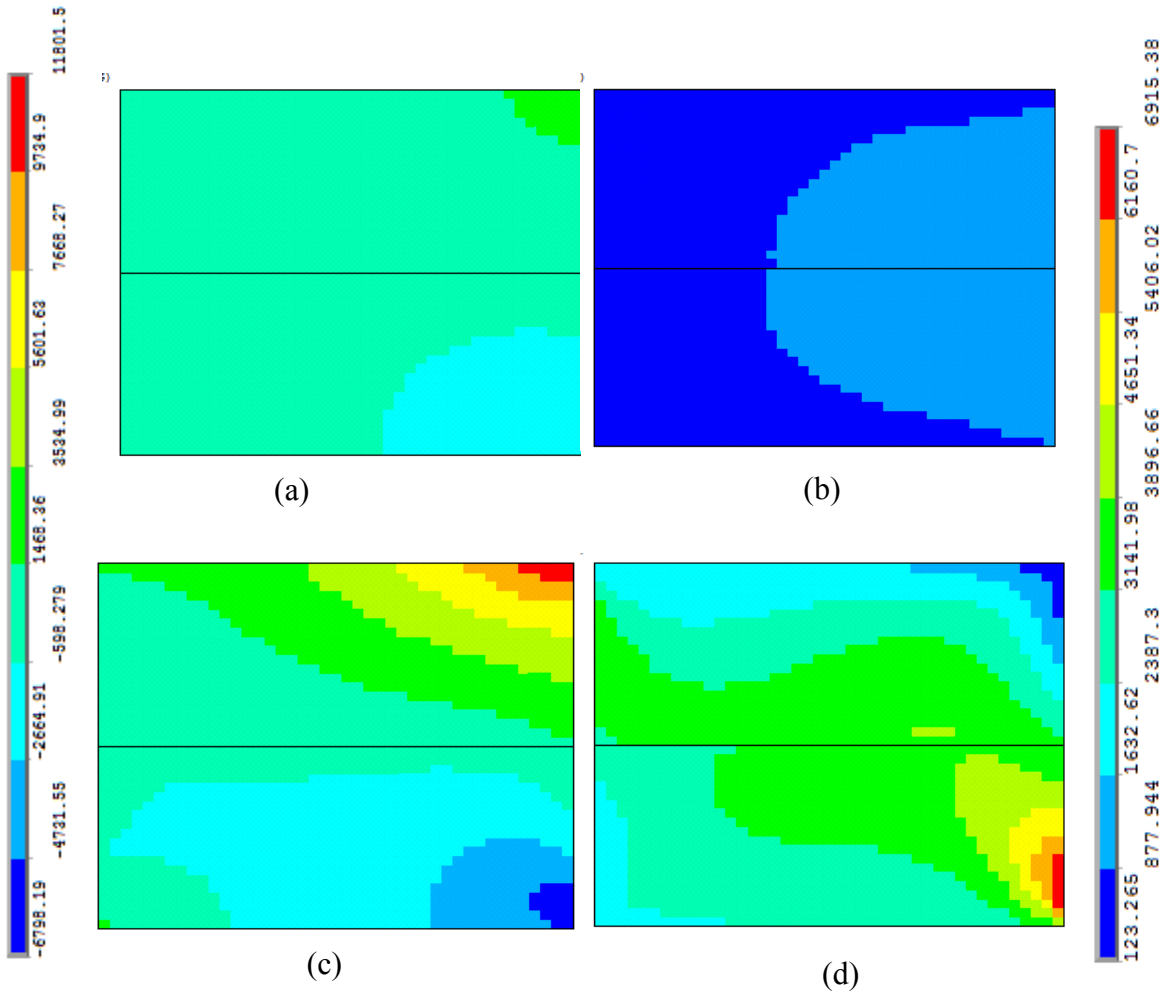

Figure 7 (a) Horizontal membrane stresses, (b) transverse shear stresses at the end of construction of outrigger and (c) horizontal membrane stresses, (d) transverse shear stresses at 4500 days of the top outrigger in kN/m^2

Figure 8 (a) and (b) below show the distribution of horizontal membrane stresses along the outrigger height at a line 1m away from the (a) column end and (b) shear wall end. Also Figures 8 (c) and (d) show and transverse shear stresses at these same locations respectively. These Figures further illustrate the increment in the membrane stresses due to increased bending moments and the transverse shear stresses with time owing to the creep and shrinkage deformations in the building column and wall elements that was discussed above. Initially both the bottom outrigger and the top outrigger are under similar stresses just after the removal of formwork, with the axial shortening of vertical elements at both outrigger levels being similar in magnitude. However at 4500 days, the stresses in the top outrigger have surpassed those at the bottom outrigger due to the higher deformation differentials at levels 39-41 compared to those at the bottom outrigger which is at levels 19-21.

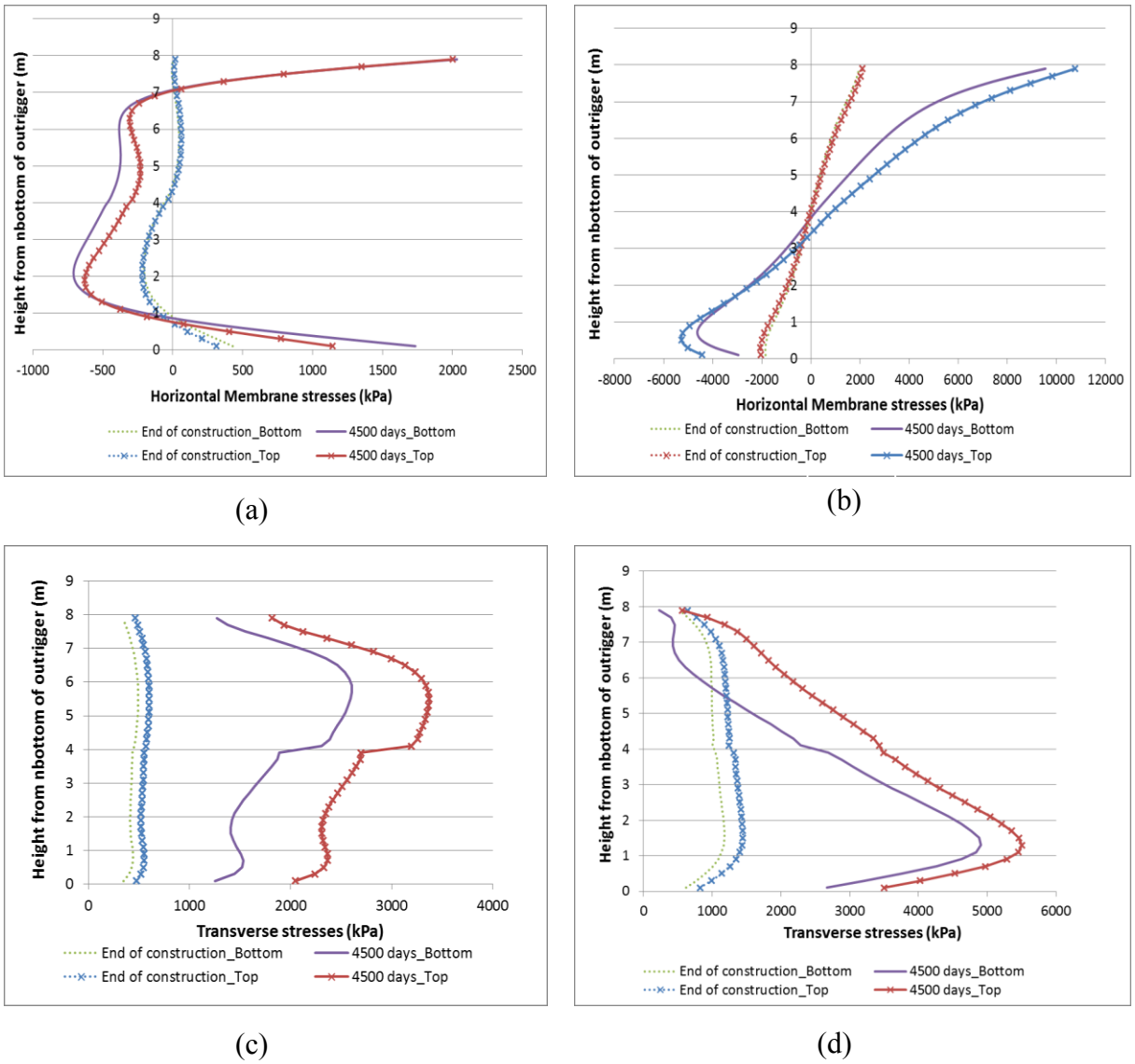

Figure 8 Horizontal membrane stresses at (a) column end, (b) shear wall end and transverse shear stresses at (c) column end, (d) shear wall end

CONCLUSIONS

A detailed analysis of a high rise building with CFST columns, reinforced concrete shear walls and outrigger belt system has been carried out using the developed method with FET to quantify the stress development in the outrigger system due to the differential shortening between columns and the shear wall structure. This modelling procedure also included the effects of reinforcement, time dependent material properties, construction sequence and interaction of outrigger and belt system with the structural frame on and during DAS. There is a 3-4 times increment in outrigger stresses from construction till the end of 4500 days due to differential axial shortening of vertical load bearing elements for the specific case studied.

The procedure can be conveniently used by practicing engineers to estimate the axial shortening of a CFST building and the expected transfer stresses in the outrigger and belt systems due to this differential shortening of the columns and shear walls. This information will provide guidance on outrigger connection timing and the need for complex control systems and enable them to make a decision on whether to design the outrigger and belt system incorporating the stress increment due to the control of differentials in displacements of linked vertical load bearing elements.

ACKNOWLEDGMENTS

The authors thankfully acknowledge the support by the High Performance Computing & Research Support Group, GP Campus, QUT and Dr. Krishna Shrestha of Balranald Shire Council, Sydney, Australia.

REFERENCES

ANSYS Inc. (2010). "Theory reference for the mechanical APDL and mechanical applications", release 13.0, USA

Bažant, ZP., and Baweja, S. (2000), "Creep and shrinkage prediction model for analysis and design of concrete structures: Modal B3". *Adam Neville Symposium*: Creep and shrinkage structural Design Effects, Al-Manaseer, A., ed., American Concrete Institute, Farmington Hills, Michigan, ACI SP-194,1-83

BSI (2004), Eurocode 2: Design of concrete structures, in *BS EN European Standards* 1992-1-1: Part 1 1: General rules and rules for buildings, European Committee for Standardization

Choi, HS., Ho, G., Joseph, L. and Mathieas, N. (2012). "Outrigger Design for High- Rise Buildings". *An output of the CTBUH Working Group*.

Geng, Y., Wang, Y., Ranzi, G., and Zhang, S. (2012). "Time-dependent behaviour of concrete-filled steel tubular columns: analytical and comparative study". *Magazine of Concrete Research*, 64(1), 55-69

Kwon, S., Kim, Y., and Kim, J. (2005). "Long-term behaviour under axial service loads of circular columns made from concrete filled steel tubes". *Magazine of Concrete Research*, 57(2), 87-99

Ma, Y.S. and Y.F. Wang. (2012). "Creep of high strength concrete filled steel tube columns". *Thin-Walled Structures*. 53(0), 91-98.

Moragaspitiya, HNP., Thambiratnam, DP., Perera, NJ. and Chan, T.H.T. (2010). "A numerical method to quantify differential axial shortening in concrete buildings". *Engineering Structures*, 32(8), 2310-2317

Samarakkody, DI., Moragaspitiya, HNP., Thambiratnam, DP. (2014). "Quantifying Differential Axial Shortening in High rise buildings with Concrete Filled Steel Tube Columns". *Proceedings of 10th fib (International Federation for Structural Concrete) International PhD Symposium in Civil Engineering*, 583-588.

Uy, B. (2001). "Static long-term effects in short concrete-filled steel box columns under sustained loading". *ACI Structural Journal*. V. 98 (No. 1), 96-104.

Wang, Y.F., Han, B., and Zhang, D. (2008). "Advances in creep of concrete filled steel tube members and structures", in *Creep, Shrinkage and Durability Mechanics of Concrete and Concrete Structures*, Two Volume Set., Taylor & Francis, 595-600.